FlowCam®

Characterizing Protein Aggregation With Orthogonal and Complementary Analytical Techniques

INTRODUCTION

Strategies for monitoring particles in biopharmaceutical formulations are central to the development and manufacturing of safe, effective drug products. Virtually all biotherapeutics will contain particles from the active pharmaceutical ingredient (API), as well as excipients like surfactants, container-closure, and impurities from manufacturing processes or product mishandling. Many of these particles and especially aggregates formed by the API are associated with degraded product quality and may be associated with increased immunogenicity or otherwise decreased product efficacy.[1–3]

A central challenge with particle analysis in biotherapeutics is the wide size range of particles that may be present[4]. Particles in these samples can be as small as a few nanometers (e.g., oligomer-sized protein aggregates, individual viruses) or large enough to be seen by the unaided eye (e.g., visible API aggregates). While several analytical techniques exist for particle monitoring, each can only analyze particles within a finite size range. Characterizing the entire particle content of a biotherapeutic sample thus requires the use of several complementary analytical techniques to cover the potentially broad size range of particles that may be present. Orthogonal techniques, or those that measure the same quantities as another technique but are based on a different measurement principle, are also often necessary in order to confirm measurements and mitigate the limitations of each individual technique. While they can be time- and sample-consuming, these multi-instrument particle monitoring strategies can provide a better understanding of a sample's particle characteristics than a single measurement alone.

ANALYTICAL METHODS FOR PARTICLE ANALYSIS

Flow imaging microscopy (FIM) is typically used as part of a particle characterization scheme in biotherapeutic research. FIM uses a combination of microfluidics and light microscopy to analyze the subvisible particles (2-100 µm in diameter) in a sample. FIM instruments can be used to measure several characteristics of subvisible particles including concentration, size, and morphology. While this information can be invaluable in biotherapeutic research, other analytical techniques are required to fully characterize the particle content of these samples.

For example, standard FIM instruments do not record information about submicron (300 nm to 2 µm) particles or nanoparticles (10-100 nm). Furthermore, light obscuration (LO), an orthogonal technique to FIM, must also be performed to meet USP <787/788> guidelines for subvisible particle monitoring.

Several FlowCam instruments have been developed that modify the basic FIM technique to extend the size range and collect measurements from multiple modalities using a single instrument and sample. For example, FlowCam Nano uses high-magnification, immersion oil-based optics to image submicron particles 300 nm to 2 µm in diameter—particles too small for standard FIM measurements, yet challenging to analyze with scattering-based techniques like dynamic light scattering (DLS). FlowCam LO performs simultaneous LO and FIM measurements on a single sample, allowing users to analyze subvisible particles with two orthogonal techniques using a single instrument and sample. The combination of FlowCam Nano and FlowCam LO is excellent for characterizing particles in biotherapeutic samples, giving researchers particle morphology information on both subvisible and submicron particles in addition to the LO data that is required for regulatory compliance. This particle information can easily be augmented with information from other complementary techniques to obtain a thorough characterization of the particles in a sample.

A PROTEIN STRESS STUDY USING COMPLIMENTARY TECHNIQUES

This white paper demonstrates how the combination of FlowCam Nano, FlowCam LO, and DLS can be used to characterize particles in biotherapeutic samples.

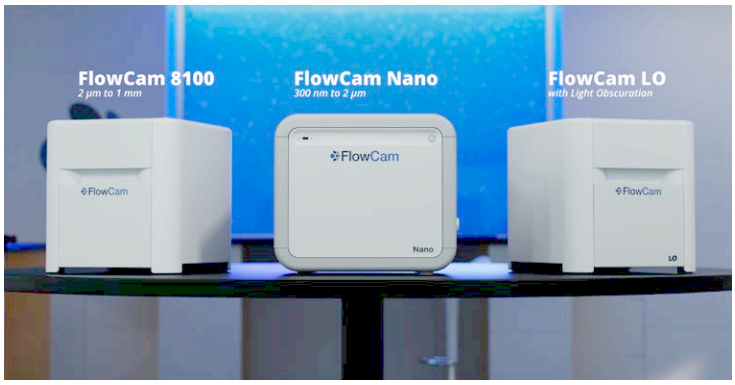

DLS was included in this analysis to measure nanoparticles that are too small to be measured by a FIM-derived technique, allowing a wide size range of particles to be accessed using only three instruments. In this study, a simple protein formulation was exposed to accelerated shaking and heat stress to promote the formation of aggregates. These two types of stresses were selected because they generate aggregates via distinct mechanisms and will likely lead to different particle size distributions following the stress.[5–7] Heat stress exposes proteins to elevated temperatures that promote protein unfolding, creating partially unfolded protein molecules that can easily generate small oligomer-sized aggregates.[6,8] Further growth and agglomeration of these smaller oligomers results in submicron- and subvisible-sized protein aggregates that FIM instruments can detect. Shaking disrupts and regenerates air-water and container-water interfaces at which proteins can adsorb and form large filmy aggregates.[9,10] It is anticipated that shaking stress will generate larger particles than heating stress as, while heating stress can only form large aggregates via growth and agglomeration from smaller nuclei aggregates, shaking stress can generate large aggregates directly.

Additionally, this study also used these particle measurement techniques to investigate the impact of surfactants on protein aggregation. Both accelerated stresses were performed with and without the presence of polysorbate 80 (PS80), a common surfactant used in protein formulations, and the resulting change in measured particle content across all three instruments was compared. It was anticipated that polysorbate would more significantly impact particles generated by accelerated shaking stress than accelerated heat stress. Polysorbate 80 and other surfactants primarily prevent aggregation by adsorbing to interfaces in the container,[9,11] mitigating protein adsorption and aggregation at that interface. As only shaking stress generates aggregates at this interface, the addition of PS80 should mitigate protein aggregation by this stress more effectively than aggregation by heat stress.

MATERIALS AND METHODS

Materials: Bovine serum albumin (BSA) powder, polysorbate 80 (PS80), and phosphate-buffered saline (PBS) were obtained from Sigma-Aldrich (St. Louis, MO). 15 µm and 700 nm Duke Standards polystyrene latex calibration beads were obtained from Thermo-Fisher Scientific (Waltham, MA). ibidi immersion oil (ibidi; Fichburg, WI) was used for FlowCam Nano measurements. Hellmanex III was obtained from Hellma (Plainview, NY). All water used in this experiment was ultrapure.

Sample Preparation: A simple protein formulation containing 1 mg/mL BSA in PBS with and without 0.1% (v/v) PS80 was prepared by mixing 12 mL PBS with 12 mg BSA powder and the necessary volume of PS80 in a 15 mL conical tube and reconstituting by gently agitating on a plate rocker for 30 minutes at room temperature. A sample containing 0.1% PS80 in 12 mL PBS without protein was also prepared and agitated on the plate rocker during reconstitution. After reconstitution, two 5 mL aliquots were taken from the three samples (BSA only, PS80 only, and BSA + PS80). Each aliquot was then exposed to one of two accelerated stress conditions: heat and agitation stress.

Shaking Stress: Samples were securely placed onto a plate rocker and agitated at the maximum speed and angle for 4 hours.

Heating Stress: Samples were placed in a 60 °C water bath for 4 hours.

Particle Analysis: Stressed samples were analyzed using three different instruments: FlowCam LO, FlowCam Nano, (Yokogawa Fluid Imaging Technologies; Scarborough, ME) and DynaPro NanoStar (Wyatt Technology; Santa Barbara, CA). These three instruments perform a total of four complementary and orthogonal analytical techniques: FIM, LO, submicron FIM, and DLS. Combined, these techniques allowed the analysis of subvisible, submicron, and nanoparticle content in each formulation following each accelerated stability stress.

FlowCam LO: FlowCam LO was used to perform simultaneous FIM and LO measurements (two orthogonal analytical methocs for subvisible particle content) on a single sample. The FIM module on the FlowCam LO unit uses a 10X objective, an 80 µm FOV flow cell, and a grayscale camera. Prior to analysis, the unit was focused with 15 µm calibration beads using the default autofocus algorithm in VisualSpreadsheet, the instrument's software, set to optimize image quality. The background intensity was also adjusted to 170 prior to measurements using the automated tools in VisualSpreadsheet. After cleaning the flow cell with 1% Hellmanex III solution, followed by ultrapure water, then PBS, particle-free PBS solution was then analyzed in LO mode to confirm that <600 particles/mL were detected via FIM and minimal particles were detected via LO.

Samples were measured in LO mode in 0.2 mL aliquots at a 0.2 mL/min flow rate. All measurements were performed using 15 dark and 15 light pixel thresholds, 4 µm distance-to-nearest-neighbors, and 3 close-hole iterations. The flow cell was cleaned before and between as described above.

Each measurement was post-processed to remove any obvious FlowCam artifacts such as blank images, stuck particles, and edge-of-flow-cell images. While air bubbles are typically removed via post-processing, many of the bubble images recorded in this analysis had visible protein aggregates adsorbed to the bubble. Bubbles were therefore not removed during post-processing to avoid removing bubbles that lacked a visible aggregate but were still stabilized via protein films.

FlowCam Nano: FlowCam Nano was used to obtain submicron particle sizing and concentrations for all six samples. FlowCam Nano instruments are equipped with a 40X objective, a 60 µm flow cell, and a grayscale camera. The instrument was focused on 700 nm calibration beads optimizing for image quality, applying fresh immersion oil when prompted during the autofocus protocol. Once cleaned, with the same procedure used for FlowCam LO, three 0.1 mL aliquots of each sample were measured at a 0.025 mL/min flow rate, in relative count mode using 20 dark and 18 light pixel thresholds, 0.1 µm distance-to-nearest-neighbors, and 3 close hole iterations.

Measurements were post-processed by filtering out particles with an edge gradient lower than 30 or a diameter outside of the instrument's size range (0.3 to 2 µm) as well as manual removal of any other artifacts observed in the dataset.

DynaPro NanoStar: DLS measurements were used to assess the nanoparticle content present in each sample. 20 µL aliquots of each sample were loaded into plastic disposable cuvettes. Samples were not filtered or otherwise processed to remove large particles that may interfere with measurements. At least three repeat measurements per sample were taken. No data filter was applied to the resulting measurements.

RESULTS

Flow Imaging Microscopy (FlowCam LO and FlowCam Nano): Two different FlowCam instruments, FlowCam LO and FlowCam Nano, were used to monitor subvisible and submicron particle content following shaking and heating stress in samples containing BSA, PS80, or both. The observed subvisible particle size distributions and sample particle images from FlowCam LO and FlowCam Nano are shown in Figures 1 and 2, respectively. Table 1 contains the particle concentrations (particles/mL) obtained from both instruments.

Shaking and heating stress without surfactant: Shaking stress appeared to produce larger, more numerous particles for all samples compared to those generated by heat stress. These results can be observed in the particle size distributions (Figures 1 and 2, histograms) and particle counts (Figure 3). Some of the observed particle content generated via shaking stress consisted of large protein aggregates adsorbed to an air bubble (Figure 1, topmost collage, boxed images); therefore, bubble images were not excluded from the FIM data in this analysis.

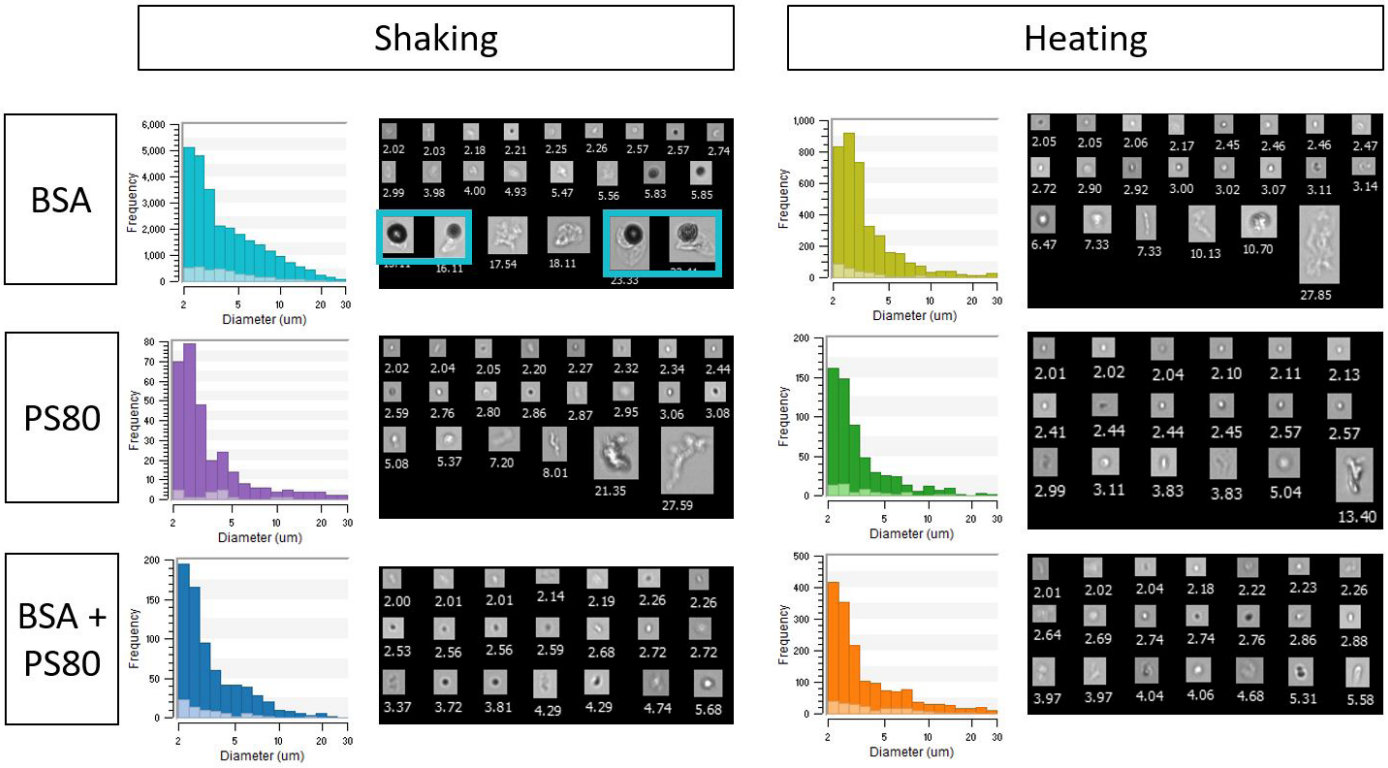

Figure 1. Subvisible particle size distributions (histograms) and sample images (collages) obtained from FlowCam LO. Dark histogram bars indicate particle sizing from FIM, light bars indicate that from LO. Boxed images are referred to in the main text. Values below each image indicate the diameter of the particle.

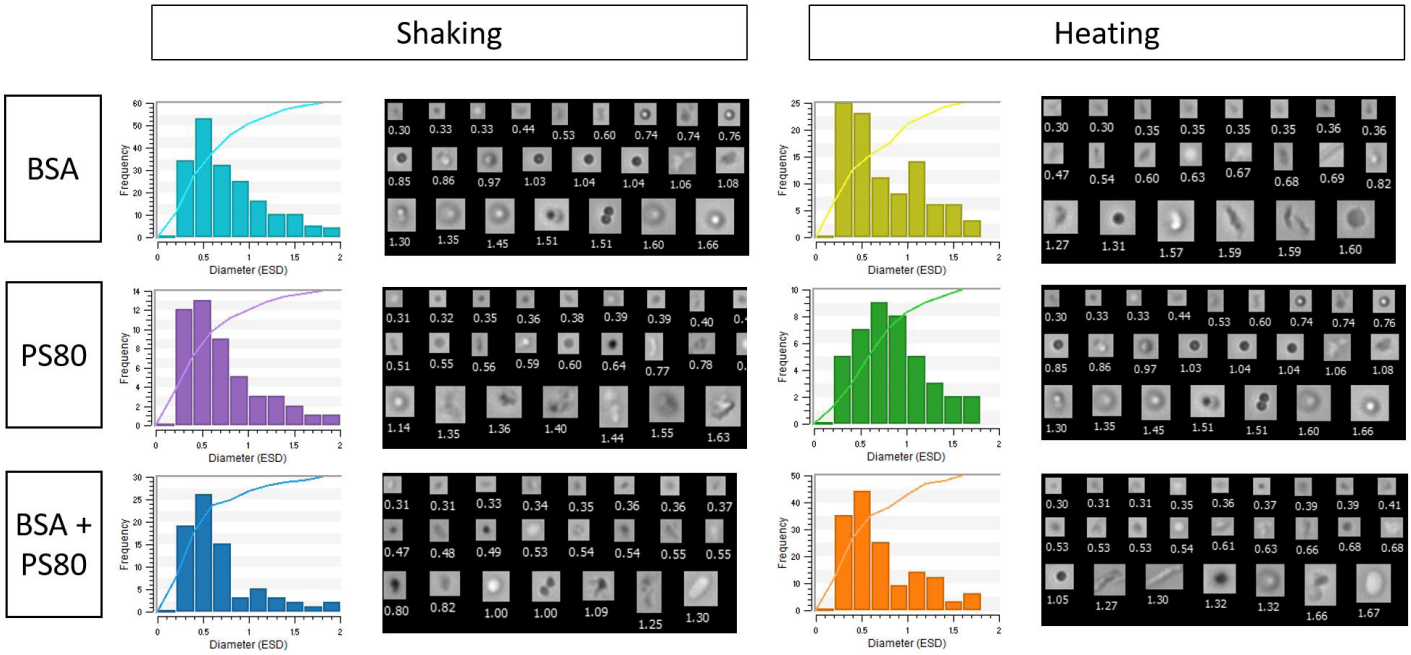

Figure 2. Submicron particle size distributions and sample particle images obtained by FlowCam Nano. Values below each image indicate the diameter of the particle.

Stresses with surfactant: The addition of PS80 to both samples generally resulted in lower particle concentrations relative to the protein-only stressed samples, with similar results reported by both FIM analysis methods. This effect was much more pronounced for the sample exposed to shaking stress than for the sample exposed to heating stress. Shaking stress generated a 97% lower subvisible particle concentration and 61% lower submicron particle concentration when performed in the presence of PS80 (Table 1). While the stressed PS80 contributed some additional particles to this sample, the reduction in protein aggregates far outweighed the particles contributed by polysorbate degradation. A decrease in particle size was also observed in the particle size distributions (Figures 1 and 2).

In contrast, the addition of polysorbate to the heat-stressed sample decreased the subvisible particle concentration by only 58% and increased the submicron particle concentration by 155%. Unlike the BSA-only samples, the BSA + PS80 sample exposed to heating stress contained higher particle concentrations than that exposed to shaking stress. Particles generated by polysorbate degradation were also more significant for this sample, although this was due in part to the lower overall particle concentrations generated by this stress. This effect is best observed in the submicron particle concentration data, as the particle concentration present in the combined BSA + PS80 sample following heat stress is roughly equal to the sum of the particle concentrations present in the BSA-only and PS80-only samples exposed to this stress. These concentrations suggest that the additional particles present in the BSA + PS80 sample compared to the BSA-only sample are due to polysorbate degradation, and that PS80 had minimal impact on submicron protein aggregates formed by heat stress. While the addition of surfactant decreased the subvisible protein aggregate concentration generated by heat stress, the impact of surfactant on aggregates generated by this mechanism was much smaller than on those generated by shaking stress.

Stress	Shaking Stress (particles / mL)			Heating Stress (particles / mL)		
Instrument	FlowCam LO		FlowCam Nano	FlowCam LO		FlowCam Nano
Technique	FIM	LO	Submicron FIM	FIM	LO	Submicron FIM
BSA	69000	6300	36000	9700	520	18000
PS80	780	33	9200	1500	95	12000
BSA + PS80	1900	130	14000	4100	380	28000

Table 1. Subvisible and submicron particle concentrations measured by FlowCam LO and FlowCam Nano.

Light Obscuration (FlowCam LO): FlowCam LO also reported subvisible particle concentrations and sizing via light obscuration (LO), an orthogonal technique to FIM. Figure 1 and Table 1 show the particle size distribution and particle counts, respectively, measured by LO. LO detected markedly lower particle concentrations (Table 1) as well as smaller particle sizes (Figure 1, light-colored, overlaid histogram bars) than FIM detected in the same aliquot of each sample. This behavior was expected due to the translucency of the protein aggregates (Figure 1 and 2, collages). LO detects and sizes particles based on the amount of light they block as particles flow between a laser and a photodiode. The semi-transparent particles in these samples only partially block light from reaching the diode, resulting in these particles being undersized if not missed entirely by LO. Despite this limitation of the LO modality, the particle sizing and concentrations reported by LO agree with the trends reported by the FIM component of FlowCam LO.

DLS: Figure 3 shows the intensity autocorrelation functions (ACFs) obtained from both BSA samples exposed to the accelerated stress conditions. As was observed with FIM, DLS also suggests that PS80 more strongly influenced particle content following shaking stress than following heat stress. The DLS measurements of the sample shaken without PS80 showed inconsistencies between replicate measurements and demonstrated significantly higher intensity autocorrelation function values at long delay times, suggesting that the sample contained high concentrations of large subvisible particles. The sample shaken with PS80 exhibited a faster, more consistent decay of the ACF to the baseline, indicating a more monomodal nanoparticle population and less subvisible particle content. In contrast, particles generated by heat stress with and without PS80 exhibit similar intensity ACFs that lack the long tail of the ACFs observed for the shaking-stressed sample, indicating reduced subvisible particle content and minimal detectable PS80 effect.

Figure 4 shows particle size distributions obtained for the BSA + PS80 samples exposed to both stresses derived from the above ACFs. While both samples exhibited some submicron and subvisible particle content, the heat stress sample contained higher concentrations of these larger particles. These results agree with the decrease in submicron and subvisible particle content observed by FIM, again suggesting that PS80 mitigated aggregation by shaking but not by heating.

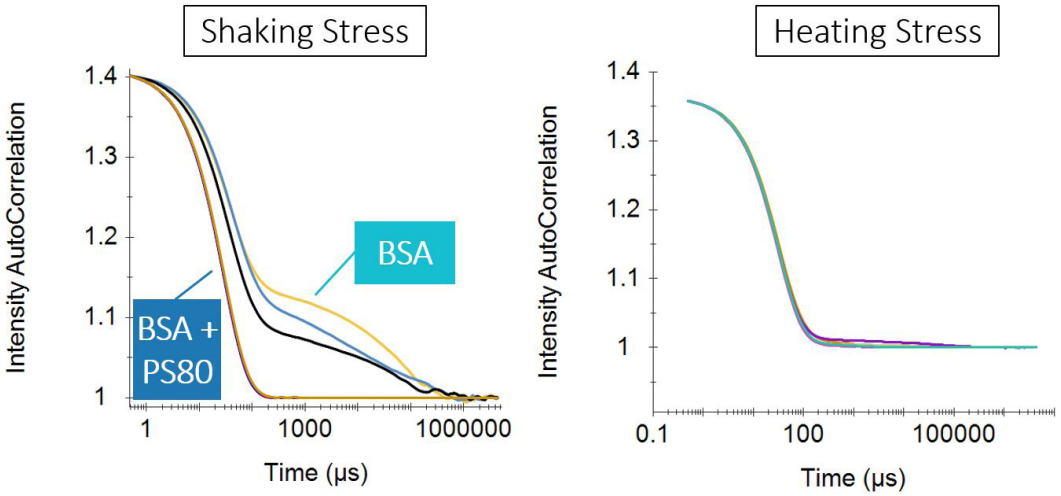

Figure 3. Autocorrelation functions (ACFs) measured by DLS from BSA samples exposed to shaking and heating stress. Boxes on the shaking sample subplot indicate which sample (BSA alone or BSA + PS80) yielded each set of three curves. These samples cannot be visually delineated in the heating sample subplot.

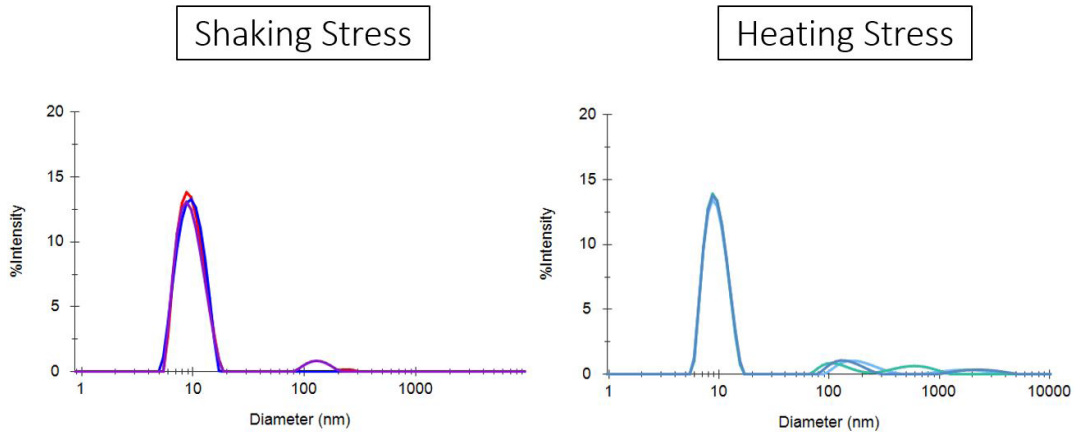

Figure 4. Particle size distributions measured by DLS for samples containing both BSA and PS80. The three curves per figure represent three replicate measurements for each sample. The main peak around 10 nm diameter represents primarily monomers and oligomers, while the peaks above 100 nm consist of larger aggregates.

DISCUSSION

The particle size and concentration measurements from all four techniques (Flow Imaging Microscopy, Submicron Flow Imaging Microscopy, Light Obscuration, and DLS) indicate similar changes in particle content between shaking and heating stresses as well as samples stressed with and without polysorbate 80. When performed on samples without PS80, shaking stress generated a larger concentration of subvisible and submicron particles than heating stress. These particles were also much larger than those generated by heating stress as evidenced by the particle size distributions from FIM and LO (Figures 1 and 2) and the ACFs from DLS (Figure 3). These trends are consistent with the expected interface-driven aggregation mechanism shaking likely induces. Since aggregation occurs at container interfaces, this stress can form large aggregates directly rather than requiring nanoparticle and submicron-sized protein aggregates to be formed first—an aggregate growth pattern likely induced by heating stress.

When stressed in the presence of PS80, the subvisible and submicron particle content generated by shaking is drastically reduced and, as a result, the nanoparticle content is measurable via DLS. In contrast, the addition of PS80 only reduced the subvisible particle concentrations generated by heating stress and had a negligible impact on the submicron- and nanoparticle-sized protein aggregates generated by the stress. These changes are consistent with the expected behavior of the surfactant; since shaking stress likely induces protein aggregation at interfaces, it was expected that the addition of surfactant would more significantly prevent protein aggregation via that stress than via heat stress.

CONCLUSIONS

This study used a combination of FlowCam LO, FlowCam Nano, and DLS measurements to compare BSA aggregate populations generated during accelerated shaking and heating stress with and without the presence of a surfactant. The observed subvisible-, submicron-, and nanoparticle content in each sample agreed with the anticipated effects on protein aggregation by the different stresses and by the presence of surfactant. These results highlight the value of using multiple orthogonal and complementary techniques to characterize particles in biotherapeutics and the breadth of particle information that is available from two FlowCam instruments alone. FlowCam LO and FlowCam Nano broaden the particle information available from traditional FIM instruments, and when combined with other common analytical techniques such as DLS, can help researchers come to a more complete understanding of the particles in their biotherapeutic samples.

REFERENCES

1. Rosenberg AS. Effects of protein aggregates: An immunologic perspective. AAPS J. 2006;8(3):E501-E507. doi:10.1208/aapsj080359

2. Joubert MK, Hokom M, Eakin C, et al. Highly aggregated antibody therapeutics can enhance the in vitro innate and late-stage T-cell immune responses. Journal of Biological Chemistry. 2012;287(30):25266-25279. doi:10.1074/jbc.M111.330902

3. Kotarek J, Stuart C, de Paoli SH, et al. Subvisible Particle Content, Formulation, and Dose of an Erythropoietin Peptide Mimetic Product Are Associated with Severe Adverse Postmarketing Events. J Pharm Sci. 2016;105(3):1023-1027. doi:10.1016/S0022-3549(15)00180-X

4. Roesch A, Zölls S, Stadler D, et al. Particles in Biopharmaceutical Formulations, Part 2: An Update on Analytical Techniques and Applications for Therapeutic Proteins, Viruses, Vaccines and Cells. J Pharm Sci. 2021;000. doi:10.1016/j.xphs.2021.12.011

5. Joubert MK, Luo Q, Nashed-Samuel Y, Wypych J, Narhi LO. Classification and characterization of therapeutic antibody aggregates. Journal of Biological Chemistry. 2011;286(28):25118-25133. doi:10.1074/jbc.M110.160457

6. Roberts CJ. Therapeutic protein aggregation: Mechanisms, design, and control. Trends Biotechnol. 2014;32(7):372-380. doi:10.1016/j.tibtech.2014.05.005

7. Calderon CP, Daniels AL, Randolph TW. Deep Convolutional Neural Network Analysis of Flow Imaging Microscopy Data to Classify Subvisible Particles in Protein Formulations. J Pharm Sci. 2018;107(4):999-1008. doi:10.1016/j.xphs.2017.12.008

8. Chi EY, Krishnan S, Randolph TW, Carpenter JF. Physical stability of proteins in aqueous solution: Mechanism and driving forces in nonnative protein aggregation. Pharm Res. 2003;20(9):1325-1336. doi:10.1023/A:1025771421906

9. Bee JS, Randolph TW, Carpenter JF, Bishop SM, Dimitrova MN. Effects of surfaces and leachables on the stability of biopharmaceuticals. J Pharm Sci. 2011;100(10):4158-4170. doi:10.1002/jps.22597

10. Bee JS, Schwartz DK, Trabelsi S, et al. Production of particles of therapeutic proteins at the air-water interface during compression/dilation cycles. Soft Matter. 2012;8(40):10329-10335. doi:10.1039/c2sm26184g

11. Grabarek AD, Bozic U, Rousel J, et al. What Makes Polysorbate Functional? Impact of Polysorbate 80 Grade and Quality on IgG Stability During Mechanical Stress. J Pharm Sci. 2020;109(1):871-880. doi:10.1016/j.xphs.2019.10.015